frontiers | Frontiers in Chemistry

TYPE Original Research
PUBLISHED 12 December 2022
DOI 10.3389/fchem.2022.1076383

OPEN ACCESS

EDITED BY
Pezhman Shiri,
Shiraz University of Medical Sciences, Iran

REVIEWED BY
Ibrahim F. Nassar,
Ain Shams University, Egypt
Atefeh Roosta,
Tianjin Institute of Industrial Biotechnology (CAS), China
Azim Ziyaei Halimehjani,
Kharazmi University, Iran

*CORRESPONDENCE
Ashraf A. Aly,
ashrafaly63@yahoo.com,
ashraf.shehata@mu.edu.eg
Bahaa G. M. Youssif,
bgyoussif@ju.edu.sa
Stefan Bräse,
stefan.braese@kit.edu

SPECIALTY SECTION
This article was submitted to Organic Chemistry, a section of the journal Frontiers in Chemistry

RECEIVED 21 October 2022
ACCEPTED 18 November 2022
PUBLISHED 12 December 2022

CITATION
Alshammari MB, Aly AA, Youssif BGM, Bräse S, Ahmad A, Brown AB, Ibrahim MAA and Mohamed AH (2022), Design and synthesis of new thiazolidinone/uracil derivatives as antiproliferative agents targeting EGFR and/or BRAF^{V600E}. *Front. Chem.* 10:1076383. doi: 10.3389/fchem.2022.1076383

Design and synthesis of new thiazolidinone/uracil derivatives as antiproliferative agents targeting EGFR and/or BRAF^{V600E}

Mohammed B. Alshammari[1], Ashraf A. Aly[2]*, Bahaa G. M. Youssif[3]*, Stefan Bräse[4,5]*, Akil Ahmad[1], Alan B. Brown[6], Mahmoud A. A. Ibrahim[7] and Asmaa H. Mohamed[2]

[1]Chemistry Department, College of Sciences and Humanities, Prince Sattam Bin Abdulaziz University, Al-Kharij, Saudi Arabia, [2]Chemistry Department, Faculty of Science, Minia University, El-Minia, Egypt, [3]Pharmaceutical Organic Chemistry Department, Faculty of Pharmacy, Assiut University, Asyut, Egypt, [4]Institute of Organic Chemistry, Karlsruher Institut fur Technologie, Karlsruhe, Germany, [5]Institute of Biological and Chemical Systems (IBCS-FMS), Karlsruhe Institute of Technology, Karlsruhe, Germany, [6]Chemistry Department, Florida Institute of Technology, Melbourne, FL, United States, [7]Computational Chemistry Laboratory, Chemistry Department, Faculty of Science, Minia University, Minia, Egypt

Thiourea derivatives of uracil were efficiently synthesized *via* the reaction of 5-aminouracil with isothiocyanates. Then, we prepared uracil-containing thiazoles *via* condensation of thioureas with diethyl/dimethyl acetylenedicarboxylates. The structures of the products were confirmed by a combination of spectral techniques including infra-red (IR), nuclear magnetic resonance (NMR), mass spectrometry (MS) and elemental analyses. A rationale for the formation of the products is presented. The newly synthesized compounds were evaluated for their *in vitro* antiproliferative activity against four cancer cell lines. The compounds tested showed promising antiproliferative activity, with GI_{50} values ranging from 1.10 μM to 10.00 μM. Compounds **3c, 5b, 5c, 5h, 5i,** and **5j** were the most potent derivatives, with GI_{50} values ranging from 1.10 μM to 1.80 μM. Compound **5b** showed potent inhibitory activity against EGFR and BRAF^{V600E} with IC_{50} of 91 ± 07 and 93 ± 08 nM, respectively, indicating that this compound could serve as a dual inhibitor of EGFR and BRAF^{V600E} with promising antiproliferative properties. Docking computations revealed the great potency of compounds **5b** and **5j** towards EGFR and BRAF^{V600E} with docking scores of −8.3 and −9.7 kcal/mol and −8.2 and −9.3 kcal/mol, respectively.

KEYWORDS

5-AU, thiourea, thiazolidinone, EGFR, B-RAF, viability, molecular modeling

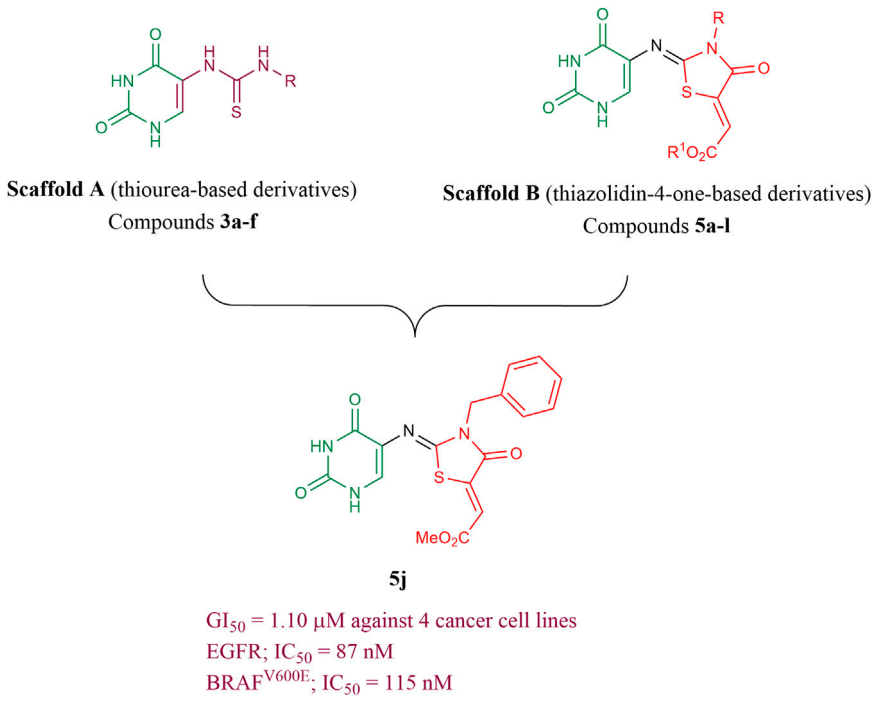

GRAPHICAL ABSTRACT

1 Introduction

Uracil compounds are promising structures in the field of drug discovery (Bouhadir et al., 2016; Putz and Dudas, 2013). Uracils substituted in position five stand out in bioactivity (Gimadieva et al., 2015), with various biological activities including antiviral properties (Palasz and Ciez, 2015), anticancer, cytotoxic (Tanase et al., 2015; Krutikov and Erkin, 2009), antimycobacterial (Isobe et al., 2003; Baraldi et al., 2002), and antitumor (Seferoglu and Ertan, 2008), to antibacterial (Lee et al., 1997). According to Rana and Ganesh (2000), 5-aminouracil (5-AU) (**compound I**, Figure 1) binds to receptors with high affinity by forming hydrogen-bonded triplexes *via* amino and carbonyl groups and a ring nitrogen. Interestingly, 5-aminouracil has antitumor, antibacterial, and antiviral properties (Zielenkiewicz et al., 2000). Furthermore, 5-AU is widely used as a cell cycle inhibitor (Oliev, 1994), as it inhibits the mitotic cycle and the incorporation of guanosine into nucleic acids (Roth and Cheng, 1982). Many thiourea derivatives demonstrate antibacterial, antifungal (Abbas et al., 2013a; El-Sharief et al., 2013), and antiviral (Abbas et al., 2013b) activities. Their ability to inhibit enzymes such as protein tyrosine kinases (PTKs) (Li et al., 2010), topoisomerase II (Huang et al., 2010), human sirtuin type proteins (Napper et al., 2005), and DNA repair synthesis (Ziegler-Skylakakis et al., 1985) may explain their anticancer activity. Some diaryl-thiourea derivatives have been reported to be EGFR inhibitors (Xiong et al., 2008). The thiourea derivative DC27 (**compound II**, Figure 1) was tested for antitumor activity in a panel of human lung carcinoma cell lines (Xiong et al., 2008). The outcomes demonstrated dose-dependent inhibition of cell proliferation, with an IC_{50} of 2.5–12.9 μM, comparable to gefitinib (1.1–15.6 μM). In contrast to gefitinib (IC_{50} = 0.018 ± 007 μM), **DC27** showed potent inhibition of EGFR with a value of 0.020 ± 005 μM. Additionally, a flow cytometry study of **DC27** (Xiong et al., 2008) induced apoptosis and G0/G1 cell cycle arrest.

The thiazolidin-4-one moiety has been proposed as a scaffold for constructing new molecules in medicinal chemistry. Positions 2, 3, and 5 of the thiazolidin-4-one ring, are amenable to modification. When modified with other substituents, thiazolidin-4-one exhibits a wide range of biological activities, including anticancer (Asati et al., 2014; Aly et al., 2020; Sharma et al., 2020). Thiazolidin-4-one hybrids were developed (Aziz et al., 2021), and their anticancer properties were tested on breast cancer (MCF-7) and lung cancer (A549) cell lines. The most effective derivative against the lung cancer (A549) cell line was compound **III** (Figure 1), with an IC_{50} value of 0.72 μM and promising EGFR inhibitory activity at a concentration of 65 nM.

In response to the previous, continuing our efforts to discover novel hybrids as inhibitors of cancer cell growth with dual targeting inhibitory action (Al-Wahaibi et al., 2020; Gomaa et al., 2022), we have now prepared two new series of hybrids (Figure 2): the dihydropyrimidine-2,4-dione/thioureas **3a-f** (**Scaffold A**) and the dihydropyrimidine-2,4-dione/thiazolidin-

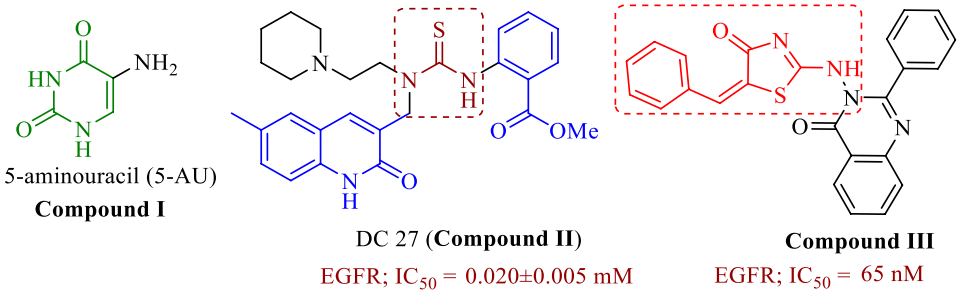

FIGURE 1
Structure of compounds **I-III**.

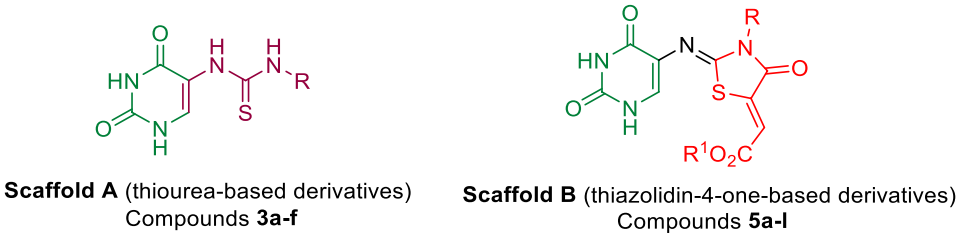

FIGURE 2
Structures of new hybrids **3a-f** and **5a-l**.

4-ones **5a-l** (**Scaffold B**). Our goal was to obtain a new antiproliferative agent that can target EGFR and/or $BRAF^{V600E}$. Using an MTT assay, the compounds were tested on a panel of four different cancer cell lines. The EGFR and BRAF enzymatic assays were used to investigate the hybrids' potential antiproliferative mechanism. A molecular docking study was conducted on the most active compounds within the target active sites of the enzymes.

2 Results and discussion

2.1 Chemistry

The syntheses of the target compounds are depicted in Schemes 1 and 2. The new thioureas **3a-f** (Scaffold A) were synthesized by the reaction of 5-aminouracil (**1**) with isothiocyanate derivatives **2a-f** in boiling methanol for 10–12 h. The structures of the target compounds **3a-f** were confirmed by elemental analyses, IR, NMR (^{1}H, ^{13}C, 2D NMR, ^{15}N), and mass spectroscopy. The ^{1}H NMR spectrum of **3d** showed six singlet signals at δ_H 11.33, 10.79, 8.69, 8.45, 7.97 and 4.69 ppm, assigned as NH-3, NH-1, NH-5a, NH-5c, CH-6 and CH_2-benzyl protons, respectively. The aromatic protons were appeared between δ_H 7.25–7.30 ppm. The ^{13}C NMR spectrum showed two carbonyl carbon (C=O) signals at δ_C 161.6 and 150.4 ppm, assigned as C-4 and C-2; there were also signals at δ_C 181.8, 134.8, and 112.7 ppm, assigned as C=S, C-6, and C-5 respectively. A non-protonated carbon at δ_C 138.9 ppm gave HMBC correlation with H-*o*, H-*m*, and H-5d; this carbon is assigned as C-*i*. The four nitrogens all gave HSQC correlation with their attached protons (Table 1; Figure 3).

A new series of pyrimidine-bearing thiazolidinones (Scaffold B, **5a-l**) was synthesized by refluxing thioureas **3a-f** with acetylenedicarboxylate derivatives **4a,b** in methanol for 4–6 h in 76–85% yields. The spectral and elemental data revealed that all **5a-l** derivatives underwent the reaction smoothly to give the respective 2,4-dioxo-1,2,3,4-tetrahydro-pyrimidin-5-yl)imino)-4-oxo-3-substituted thiazolidin-5-ylidene)-acetates.

The ^{1}H NMR spectra showed the disappearance of NH-5a signal of the thiourea in molecule **3**. For example, **5d** formed by the reaction of compound **3d** with diethyl acetylenedicarboxylate (**4a**). The signals of the ethoxy group were distinctive at δ_H 4.23 (H-5c′) and 1.25 (H-5d′), δ_C 61.5 (C-5c′) and 13.9 ppm (C-5d′): H-5c′ gave HMBC correlation with a carbon at δ_C 165.3 ppm, assigned as C-5b'. C-5b′ also gave HMBC correlation with a

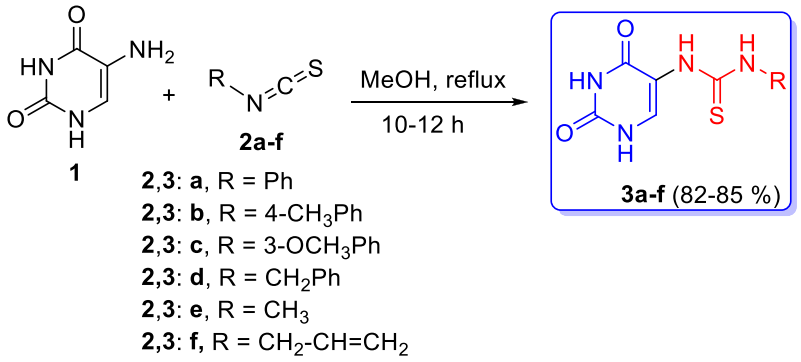

2,3: **a**, R = Ph
2,3: **b**, R = 4-CH_3Ph
2,3: **c**, R = 3-OCH_3Ph
2,3: **d**, R = CH_2Ph
2,3: **e**, R = CH_3
2,3: **f**, R = CH_2-CH=CH_2

SCHEME 1
Synthesis of thiourea-based hybrids **3a-f**.

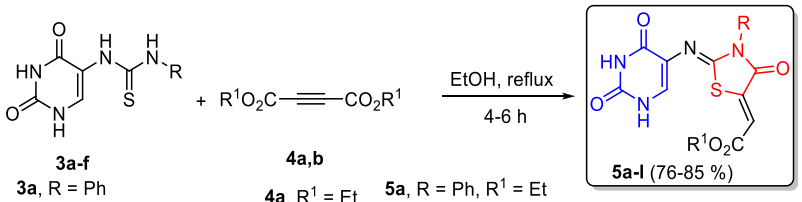

3a-f
3a, R = Ph
3b, R = 4-CH_3Ph
3c, R = 3-OCH_3Ph
3d, R = CH_2Ph
3e, R = CH_3
3f, R = CH_2-CH=CH_2

4a,b
4a, R^1 = Et
4b, R^1 = Me

5a, R = Ph, R^1 = Et
5b, R = 4-CH_3Ph, R^1 = Et
5c, R = 3-OCH_3Ph, R^1 = Et
5d, R = CH_2Ph, R^1 = Et
5e, R = CH_3, R^1 = Et
5f, R = CH_2-CH=CH_2, R^1 = Et
5g, R = Ph, R^1 = Me
5h, R = 4-CH_3Ph, R^1 = Me
5i, R = 3-OCH_3Ph, R^1 = Me
5j, R = CH_2Ph, R^1 = Me
5k, R = CH_3, R^1 = Me
5l, R = CH_2-CH=CH_2, R^1 = Me

SCHEME 2
Synthesis of thiazolidin-4-ones **5a-l**.

proton at δ_H 6.77 ppm, assigned as H-5a'; its attached carbon appeared at δ_C 115.2 ppm. H-5a′ also gave HMBC correlation with carbons at δ_C 140.5 and 164.1 ppm; these carbons are assigned as C-5′ and C-4′, respectively on chemical-shift grounds, confirmed by HMBC correlation between C-4′ and the singlet of CH_2-benzyl at δ_H 5.02, assigned as H-3a'. H-3a′ gave HSQC correlation with its attached carbon at δ_C 45.5; H-3a′ also gave HMBC correlation with a nitrogen at δ_N 160.4, assigned as *N*-3′, and with a carbon at δ_C 153.0, assigned as C-2'. H-6 gave HMBC correlation with an sp^2 nitrogen at δ_N 244.8 ppm, assigned as *N*-5a, and with carbon at δ_C 159.6. The IR spectrum of **5d** showed strong absorption bands between ν = 3150 (NH), 2975 (Ar-CH), 1687 (CO), 1647 (C=N) and 1510 cm^{-1} (C=C). The mass spectrum and elemental analyses of **5d** agreed with the assigned structure (Table 2; Figure 4).

On reacting compounds **3a-f** with dimethyl acetylene dicarboxylate (**4b**), methyl (*Z*)-2-((*Z*)-2-((2,4-dioxo-1,2,3,4-tetrahydropyrimidin-5-yl)imino)-3-yl-4-oxothiazolidin-5-ylidene) acetates **5g-l** were formed. The structure assignments of **5g–I** were delineated from their spectroscopic properties and elemental analyses. The molecular structure of **5j**, for example, was supported as follows: the molecular formula of **5j** ($C_{17}H_{14}N_4O_5S$) corresponded to one molecule of **3d** and one molecule of dimethyl acetylenedicarboxylate (**4b**) less one molecule of methanol, giving rise to the ion *m/z* = 386. The NMR spectra of **5j** closely resembled those of **5d,** with a methyl ester replacing the ethyl ester (Table 3).

We recently reacted thioureas bearing a [2.2]paracyclophane moiety with diethyl acetylene-dicarboxylate (**4a**) to form thiazolidinones (Alshammari et al., 2022). An X-ray crystal

TABLE 1 NMR spectroscopy of compound 3d.

^{1}H NMR (DMSO-d_6)	^{1}H–^{1}H COSY		Assignment
11.33 (bs; 1H)			NH-3
10.79 (bs; 1H)			NH-1
8.69 (bs; 1H)			NH-5a
8.45 (b; 1H)	4.69		NH-5c
7.97 (b; 1H)			H-6
7.30 (m; 4H)			H-*o*, *m*
7.25 (m; 1H)			H-*p*
4.69 (s; 2H)	8.45		H-5d
^{13}C NMR (DMSO-d_6)	HSQC	HMBC	Assignment
181.8		4.69	C-5b
161.6			C-4
150.4			C-2
138.9		7.30, 4.69	C-*i*
134.8			C-6
128.1	7.30	7.30	C-*m*
127.2	7.30	7.30, 4.69	C-*o*
126.7	7.25	7.30	C-*p*
112.7		11.33	C-5
47.2	4.69	7.30, 4.69	C-5d
^{15}N NMR (DMSO-d_6)	HSQC	HMBC	Assignment
157.1	11.33		N-3
127.7	10.79		N-1
118.0	8.45		N-5c
107.8	8.69		N-5a

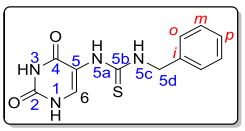

FIGURE 3
Distinctive carbons and hydrogens for compound **3d**.

structure showed the C=N and C=C double bonds to both have (*Z*) stereochemistry (Figure 5); in the current series **5a-l,** we assign the C=N and C=C bonds as both (*Z*) by analogy with our earlier work. Further evidence was based upon the suggestion that there is a resonance stabilized by the hydrogen bond formed *via* the oxygen of the carbonyl group and the exo-cyclic hydrogen as shown in Figure 6.

The rationale for forming **5a-l** begins with conjugate attack by the sulfur lone-pair of the thione group in **3a-f** on the triple bond of **4a,b** by the nitrogen lone pairs to generate the zwitterions **6a-l**. Subsequently, proton migration would give

TABLE 2 NMR spectroscopy of compound 5d.

^{1}H NMR (DMSO-d_6)	^{1}H–^{1}H COSY	Assignment
11.41 (bs; 1H)		NH-3
10.96 (bs; 1H)	7.30	NH-1
7.40 (d, *J* = 6.9; 2H)	7.33, 5.02	H-*o*
7.33 (dd, *J* = 7.5, 6.8; 2H)	7.40, 7.30	H-*m*
7.30 (m; 2H)	10.96, 7.33	H-*p*
6.77 (s; 1H)		H-5a′
5.02 (s; 2H)	7.40	H-3a′
4.23 (q, *J* = 7.1; 2H)	1.25	H-5c′
1.25 (t, *J* = 7.1; 3H)	4.23	H-5d′

^{13}C NMR (DMSO-d_6)	HSQC	HMBC	Assignment
165.3		6.77, 4.23	C-5b′
164.1		6.77, 5.02	C-4′
159.6		7.30	C-4
153.0		7.30, 5.02	C-2′
150.4		7.30	C-2
140.5		6.77	C-5′
135.5		7.33, 5.02	C-*i*
131.3	7.30	7.33, 7.30	C-*o*
128.4	7.33	7.40, 7.33, 5.02	C-*m*
127.8	7.40	7.40, 7.33	C-*p*
127.6	7.30		C-6
121.1		11.41	C-5
115.2	6.77	6.77	C-5a′
61.5	4.23	1.25	C-5c′
45.5	5.02	7.40, 5.02	C-3a′
13.9	1.25	4.23, 1.25	C-5d′
^{15}N MR (DMSO-d_6)	HSQC	HMBC	Assignment
244.8		7.30	N-5a
160.4		5.02	N-3′
157.3	11.41	11.41	N-3
127.6	10.96	7.30	N-1

intermediates **7a-l** (Scheme 3). Finally, the lone pair of the nitrogen atom in the intermediate **7a-l** would attack the carbonyl group of the same compound, which is accompanied by the elimination of an alcohol molecule to give the final product **5a-l** (Scheme 3).

2.2 Biology

2.2.1 Cell viability assay

To test the viability of new compounds, the human mammary gland epithelial (MCF-10A) cell line was used (Youssif et al., 2019; Mahmoud et al., 2022). MCF-10A cells were incubated with compounds **3a-f** and **5a-l** for 4 days before being tested for

10.3389/fchem.2022.1076383

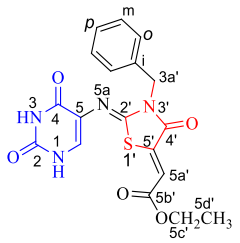

FIGURE 4
Distinctive carbons and hydrogens for compound **5d**.

viability using the MTT assay. Table 4 shows that none of the compounds tested exhibited cytotoxic effects, and cell viability was greater than 86% for the compounds tested at 50 μM.

2.2.2 Antiproliferative assay

Using the MTT assay (Abdelrahman et al., 2017; El-Sherief et al., 2018) and doxorubicin as the reference drug, **3a-f** and **5a-l** were tested for antiproliferative activity against four human cancer cell lines: Panc-1 (pancreas cancer cell line), MCF-7 (breast cancer cell line), HT-29 (colon cancer cell line), and A-549 (epithelial cancer cell line). The median inhibitory concentrations (IC_{50}) are shown in Table 4.

The 18 newly synthesized compounds have two main backbones: thiourea-based derivatives, Scaffold A (**3a-f**), and thiazolidin-4-ones, Scaffold B (**5a-l**). The compounds tested showed promising antiproliferative activity, with GI_{50} values ranging from 1.10 μM to 10.00 μM. Compounds **3c**, **5b**, **5c, 5h, 5i,** and **5j** were the most potent derivatives of both backbones, with GI_{50} values ranging from 1.10 μM to 1.80 μM. Compound **5j** (R = benzyl, R^1 = Me; thiazolidin-4-one backbone) demonstrated the most potent activity, with a GI_{50} value of 1.10 μM, comparable to the reference doxorubicin (GI_{50} = 1.10 μM) and even more potent than doxorubicin against A-549 and Panc-1 cancer cell lines, as shown in Table 4. Compound **5d** (R = benzyl, R^1 = Et; thiazolidin-4-one backbone) showed a GI_{50} of 5.15 μM, which is approximately 5-fold less potent than compound **5j**, indicating the importance of methyl ester for antiproliferative action, which is more tolerated than ethyl ester. Furthermore, compound **3d** (R = benzyl; thiourea-based backbone) showed moderate antiproliferative activity with a GI_{50} value of 4.15 μM, four times less active than compound **5j** of thiazolidin-4-one backbone, indicating that thiazolidin-4-one backbone is more tolerated for antiproliferative action than thiourea one.

Compound **5b** (R = *p*-CH_3-Ph, R^1 = Et; thiazolidin-4-one backbone) ranks second in activity, with a GI_{50} of 1.30 μM, which is 1.2-fold less potent than compounds **5j** and doxorubicin. Compound **5b** had the same potency as doxorubicin against both A-549 and Panc-1 cancer cell lines, with IC_{50} values of 1.20 μM and 1.40 μM, respectively. **5b** was found to be more potent than its methyl ester derivative, compound **5h** (R = *p*-CH_3-Ph, R^1 = Me; thiazolidin-4-one backbone), which had a GI_{50} value of 1.65 μM (Table 1).

Once again, the methyl ester derivative compound **5i** (R = *m*-OCH_3-Ph, R^1 = Me; thiazolidin-4-one backbone) outperformed the ethyl ester derivative **5c** (R = *m*-OCH_3-Ph, R^1 = Et; thiazolidin-4-one backbone) with GI_{50} values of 1.35 μM and 1.70 μM against the four cancer cell lines, respectively. Moreover, the antiproliferative activity of compounds **5i** and **5c** (thiazolidin-4-one-based derivatives; R = *m*-OMe-Ph) was comparable to that of compound **5b** (thiazolidin-4-one-based derivatives; R = *p*-Me-Ph), indicating that both *m*-OMe-Ph and *p*-Me-Ph

TABLE 3 NMR spectroscopy of compound 5j.

^{1}H NMR (DMSO-d_6)	^{1}H–^{1}H COSY	Assignment
11.41 (bs; 1H)		NH-3
10.95 (b; 1H)	7.30	NH-1
7.41 (d, *J* = 7.0; 2H)	7.34, 5.03	H-*o*
7.34 (dd, *J* = 7.4, 6.8; 2H)	7.41, 7.29	H-*m*
7.30 (s; 1H)	10.95	H-6
7.29 (t, *J* = 6.5; 1H)	7.34	H-*p*
6.81 (s; 1H)		H-5a′
5.03 (s; 2H)		H-3a′
3.77 (s; 3H)		H-5c′

^{13}C NMR (DMSO-d_6)	HSQC	HMBC	Assignment
165.7		6.81, 3.77	C-5b′
164.2		6.81, 5.03	C-2′
159.5		11.51, 7.30	C-4
153.0		5.03	C-4′
150.4		7.30	C-2
140.7		6.81	C-5′
135.6		7.34, 5.03	C-*i*
131.4	7.30		C-6
128.5	7.34	7.34	C-*m*
127.9	7.41	7.41, 7.29	C-*o*
127.6	7.29	7.41, 7.29, 5.03	C-*p*
120.7		11.41	C-5
115.4	6.81	6.81	C-5a′
52.6	3.77	3.77	C-5c′
45.6	5.03	7.41, 5.03	C-3a′

^{15}N NMR (DMSO-d_6)	HSQC	HMBC	Assignment
160.9	11.41	5.03	N-3′
158.0	11.41	11.41	N-3
127.2	10.95	11.41	N-1

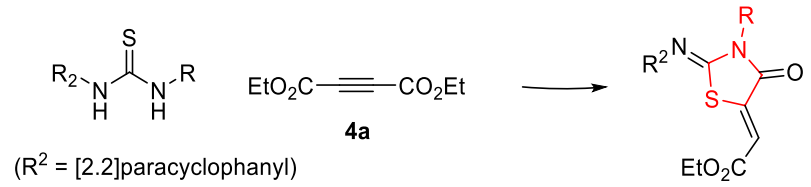

FIGURE 5
Stereochemistry of **5a-l**.

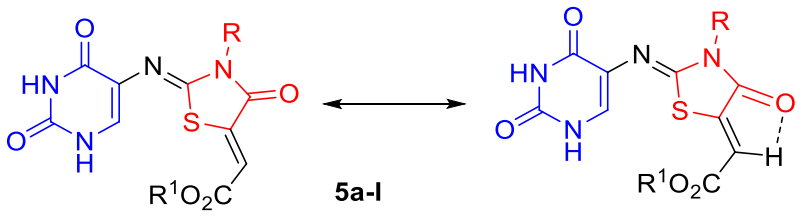

FIGURE 6
Resonance stabilized compounds **5a-l**.

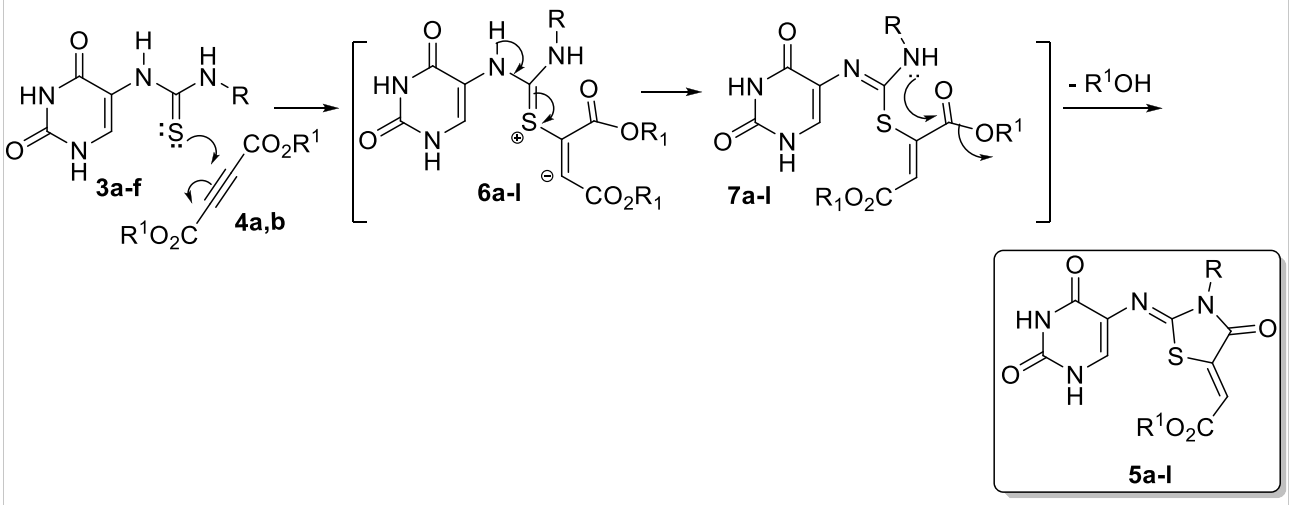

SCHEME 3
Suggested mechanism for the formation of compounds **5a-l**.

groups are well tolerated. Compound **3c** (R = *m*-OCH_3-Ph; thiourea-based backbone) was the only thiourea-based derivative with a GI_{50} less than 2 μM (GI_{50} = 1.80 μM), confirming that thiazolidin-4-one based derivatives have higher inhibitory activity against the tested cancer cell line than thiourea-based derivatives.

2.2.3 EGFR inhibitory assay

The six most potent antiproliferative derivatives (**3c, 5b, 5c, 5h, 5i,** and **5j**) were further tested for their inhibitory action against EGFR (Mohamed et al., 2021) as a potential target for their antiproliferative activity. Table 5; Figure 7 shows the results as IC_{50} values.

10.3389/fchem.2022.1076383

TABLE 4 Antiproliferative activity of compounds 3a-f, 5a-l, and Doxorubicin.

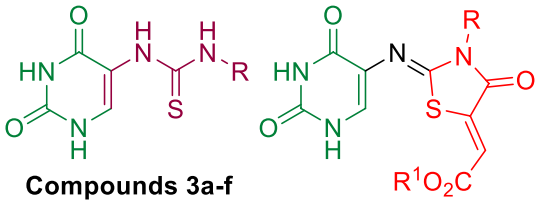

Compd.	Cell viability %	Antiproliferative activity IC_{50} ± SEM (nM)				
		A-549	MCF-7	Panc-1	HT-29	Average
3a	**86**	8.90 ± 0.80	8.50 ± 0.80	8.80 ± 0.80	9.10 ± 0.80	8.80
3b	**87**	3.70 ± 0.30	3.60 ± 0.30	4.10 ± 0.30	3.90 ± 0.30	3.80
3c	**89**	1.80 ± 0.20	1.40 ± 0.10	2.10 ± 0.20	2.10 ± 0.20	1.85
3d	**91**	4.10 ± 0.40	3.90 ± 0.40	4.30 ± 0.40	4.30 ± 0.40	4.15
3e	**89**	9.70 ± 0.80	9.60 ± 0.80	9.80 ± 0.80	10.80 ± 0.90	10.00
3f	**89**	3.80 ± 0.30	3.70 ± 0.30	3.90 ± 0.30	4.10 ± 0.30	3.90
5a	**91**	3.50 ± 0.30	3.10 ± 0.30	3.30 ± 0.30	3.90 ± 0.30	3.45
5b	**92**	1.20 ± 0.10	1.10 ± 0.10	1.40 ± 0.10	1.40 ± 0.10	1.30
5c	**96**	1.50 ± 0.10	1.60 ± 0.10	1.90 ± 0.20	1.80 ± 0.10	1.70
5d	**86**	4.90 ± 0.50	4.70 ± 0.40	5.50 ± 0.50	5.50 ± 0.50	5.15
5e	**86**	7.20 ± 0.60	6.70 ± 0.70	7.30 ± 0.70	7.20 ± 0.70	7.10
5f	**89**	8.20 ± 0.70	7.90 ± 0.70	8.80 ± 0.70	8.90 ± 0.70	8.50
5g	**87**	2.70 ± 0.20	2.20 ± 0.20	2.90 ± 0.20	2.20 ± 0.20	2.50
5h	**92**	1.40 ± 0.10	1.70 ± 0.10	1.80 ± 0.10	1.70 ± 0.10	1.65
5i	**89**	1.30 ± 0.10	1.00 ± 0.08	1.50 ± 0.10	1.60 ± 0.10	1.35
5j	**89**	1.10 ± 0.10	0.90 ± 0.10	1.20 ± 0.10	1.20 ± 0.10	1.10
5k	**89**	5.70 ± 0.60	5.10 ± 0.50	5.90 ± 0.50	6.20 ± 0.60	5.70
5l	**86**	6.00 ± 0.60	6.50 ± 0.60	6.40 ± 0.60	6.60 ± 0.60	6.40
Doxorubicin	-	1.20 ± 0.10	0.90 ± 0.10	1.40 ± 0.10	1.00 ± 0.10	1.10

TABLE 5 IC_{50} of compounds 3c, 5b, 5c, 5h, 5i, and 5j against EGFR and $BRAF^{V600E}$.

Compd.	EGFR inhibition IC_{50} ± SEM (nM)	$BRAF^{V600E}$ inhibition IC_{50} ± SEM (nM)
3c	125 ± 11	148 ± 12
5b	91 ± 07	93 ± 08
5c	115 ± 10	107 ± 10
5h	112 ± 10	137 ± 12
5i	96 ± 07	122 ± 12
5j	87 ± 05	115 ± 12
Erlotinib	80 ± 05	60 ± 05

The findings of this test are consistent with the findings of the antiproliferative assay, in which compound **5j** (R = benzyl, R^1 = Me; thiazolidin-4-one backbone), the most potent antiproliferative, demonstrated the highest inhibitory activity against EGFR with an IC_{50} value of 87 ± 05 nM, which is very close to that of the reference erlotinib (IC_{50} = 80 ± 05 nM). Compounds **5b** (R = *p*-CH_3-Ph, R^1 = Et; thiazolidin-4-one backbone) and **5i** (R = *m*-OCH_3-Ph, R^1 = Me; thiazolidin-4-one backbone) rank second and third in activity with IC_{50} values of 91 ± 07 nM

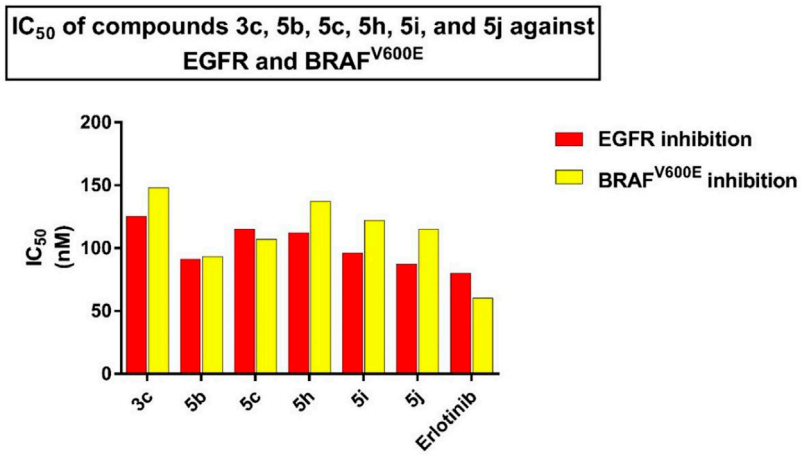

FIGURE 7
IC_{50} of compounds **3c**, **5b**, **5c**, **5h**, **5i**, and **5j** against EGFR and $BRAF^{V600E}$.

and 97 ± 07 nM, respectively. Compound **3c** (R = *m*-OCH_3-Ph; thiourea-based backbone) was the least potent of the six compounds tested, with an IC_{50} value of 125 ± 11 nM, making it 1.6-fold less potent than erlotinib. Based on the results of this assay, compounds **5b**, **5i**, and **5j** showed promising antiproliferative activity and have the potential to act as EGFR inhibitors.

2.2.4 $BRAF^{V600E}$ inhibitory assay

Compounds **3c, 5b, 5c, 5h, 5i,** and **5j** were further tested for their inhibitory action against mutant BRAF (Mohassab, A. M., et al., 2021), and results were cited in Table 5 and Figure 7 as IC_{50} values. The tested compounds showed moderate inhibitory activity against the tested mutant BRAF, with IC_{50} values ranging from 93 nM to 148 nM and were all less potent than the reference erlotinib (IC_{50} = 60 ± 05 nM). Compound **5b** (R = *p*-CH_3-Ph, R^1 = Et; thiazolidin-4-one backbone) was the most potent derivative as $BRAF^{V600E}$ inhibitor with IC_{50} of 93 ± 08 nM indicating that this compound could serve as a dual inhibitor of EGFR and $BRAF^{V600E}$ with promising antiproliferative properties.

2.3 Molecular docking

AutoDock4.2.6 software was utilized to carry out all docking computations (Morris et al., 2009). The crystal structures of EGFR and $BRAF^{V600E}$ with PDB accession codes: 1M17 (Stamos et al., 2002) and 3OG7 (Bollag et al., 2010), respectively, were obtained and utilized as templates for all docking computations. The pdbqt file of both EGFR and $BRAF^{V600E}$ was prepared as described by Ibrahim et al. (2022a) and Ibrahim et al. (2022b). The Lamarckian genetic algorithm (LGA) opted for inhibitor conformational searching and docking parameters involving 25,000,000 energy evaluations and 250 genetic algorithm runs. The rest parameters were kept as default. A grid box with 50 Å × 50 Å × 50 Å in the *x*, *y*, and *z* directions were utilized to include the binding pocket of EGFR and $BRAF^{V600E}$. The grid maps with a spacing of 0.375 Å were generated utilizing the AUTOGRID program (Goodford, 1985). The grid was positioned at the center of the active sites of EGFR and $BRAF^{V600E}$. The molecular interactions were depicted using the BIOVIA Discovery Studio Visualizer 2020 (Dassault Systèmes, 2019).

To reveal the binding modes of the synthesized compounds with the active site of the EGFR and $BRAF^{V600E}$, docking computations were performed. Validation of the AUTODOCK4.2.6 software with the employed parameters was initially executed according to the accessible experimental data. The co-crystallized inhibitors–namely 4-anilinoquinazoline and PLX4032—with the EGFR and $BRAF^{V600E}$ were redocked and compared to the native structures (PDB ID; 1M17 and 3OG7, respectively) (Figure 8). As shown in Figure 8, the predicted docking poses were approximately identical to the co-crystallized structures, having 0.20 and 0.18 Å RMSD compared to the co-crystallized conformations of 4-anilinoquinazoline and PLX4032, respectively (Figure 8). In essence, the utilized docking protocol could be applied to foretell the correct binding mode of ligands with the targeted receptors.

Based on the validated performance of AUTODOCK4.2.6 software, it was utilized to predict the docking scores and binding features of the synthesized compounds against EGFR and $BRAF^{V600E}$. The anticipated

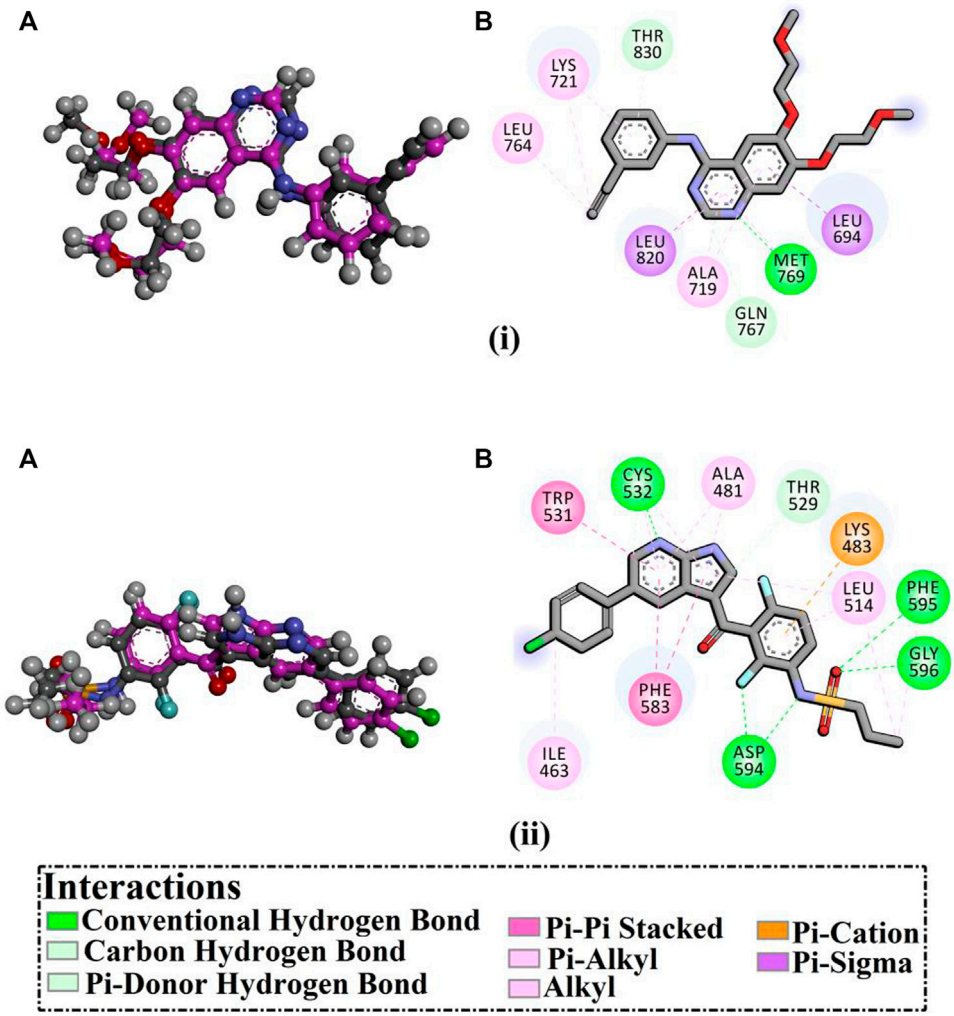

FIGURE 8
(A) 3D molecular interactions of the predicted binding modes (in purple) and the native structures (in gray) and **(B)** 2D representations of the portended binding modes of (i) 4-anilinoquinazoline with EGFR and (ii) PLX4032 with $BRAF^{V600E}$.

binding features and docking scores are compiled in Supplementary Table S1. Based on the data enrolled in Supplementary Table S1, all investigated molecules demonstrated superior docking scores against EGFR and $BRAF^{V600E}$, with values ranging from −8.0 to −8.3 and from −9.1 to −9.7 kcal/mol, respectively. The special binding affinities against EGFR and $BRAF^{V600E}$ may be attributed to their capability of exhibiting a diversity of H-bonds, π-based, hydrophobic, and vdW interactions with the most important amino acids inside the binding pockets of EGFR and $BRAF^{V600E}$. Comparing the docking results demonstrated that compounds **5b** and **5j** unveiled promising docking scores against EGFR and $BRAF^{V600E}$ with values of −8.3 and −9.7 kcal/mol and −8.2 and −9.3 kcal/mol, respectively. More exactly, compound **5b** exhibited four and five hydrogen bonds with LYS721 (2.14 Å), MET769 (2.09, 2.43 Å), and GLY772 (2.83 Å) and THR529 (2.24, 3.03 Å), CYS532 (2.13 Å), ASN580 (2.65 Å), and ASN581 (2.12 Å) within the binding pockets of EGFR and $BRAF^{V600E}$, respectively (Supplementary Table S1; Figure 9).

Compound **5j** formed six and seven hydrogen bonds with LYS721 (1.63, 2.96 Å), THR766 (2.44, 2.84 Å), GLN767 (2.29 Å), and MET769 (1.82 Å) and LYS483 (1.86 Å), THR529 (2.52 Å), ASN581 (1.97 Å), ASP594 (2.08, 2.20 Å), PHE595 (2.95 Å), and GLY596 (2.39 Å) inside the binding sites of EGFR and $BRAF^{V600E}$, respectively (Supplementary Table S1; Figure 9).

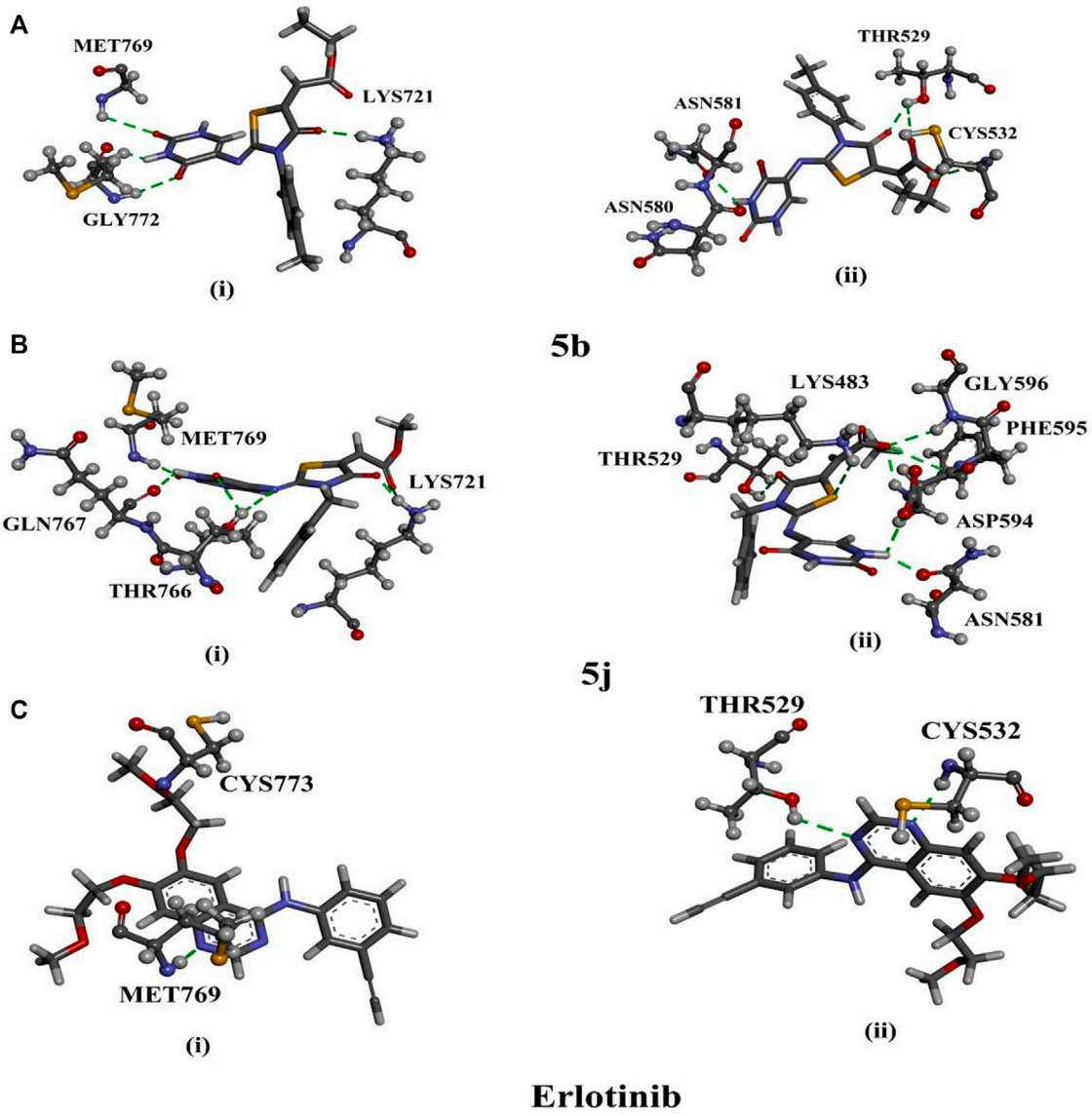

FIGURE 9
3D representations of interactions of compounds **(A) 5b**, **(B) 5j**, and **(C)** erlotinib with key residues of (i) EGFR and (ii) $BRAF^{V600E}$.

Erlotinib, a positive control, manifested good docking scores towards EGFR and $BRAF^{V600E}$ with values of −8.6 and −8.4 kcal/mol, respectively (Supplementary Table S1). As illuminated in Figure 9, erlotinib demonstrated two hydrogen bonds with MET769 (1.62 Å) and CYS773 (1.91 Å) within the active site of EGFR and two hydrogen bonds with THR529 (2.07 Å) and CYS532 (2.02 Å) within the active site of $BRAF^{V600E}$ (Supplementary Table S1). A docking comparison of erlotinib with compounds **5b** and **5j** exposed competing docking scores proposing the *in-silico* perspective of the three molecules as EGFR and $BRAF^{V600E}$ inhibitors.

3 Experimental

Instrumentation: See Supplementary Appendix SA.

3.1 General procedure for the synthesis of compounds 3a-f

Compounds **3a-f** were synthesized by refluxing of 5-aminouracil (**1**, 10 mmol) and different isothiocyanates **2a-f** (1.2 mmol) in methanol (50 ml) and the presence of a

few drops of triethylamine (0.5 ml) as a catalyst for 10–12 h. The resulting solid was filtered and recrystallized from DMF.

3.1.1 1-(2,4-Dioxo-1,2,3,4-tetrahydropyrimidin-5-yl)-3-phenylthiourea (3a)

Yield: 84%; mp 340–342°C, IR (KBr): υ_{max}/cm^{-1} = 3165 (NH), 2991 (Ar-CH), 1735 (CO), 1669 (CO), 1574 (C=C), 1330, 1208 (C=S). ^{1}H NMR (DMSO-d_6): δ_H = 7.15 (t, 1H, J = 7.4 Hz, Ar-H), 7.34 (dd, 2H, J = 8.1, 7.6 Hz, Ar-H), 7.48 (d, 2H, J = 7.8 Hz, Ar-H), 11.41 (bs, 1H, ^{3}NH), 8.16 (bs, 1H, CH-6), 8.87 (s, 1H, ^{5a}NH), 9.98 (bs, 1H, ^{5c}NH), 10.82 ppm (bs, 1H, ^{1}NH), ^{13}C NMR (DMSO-d_6): δ_C = 113.2 (C-5), 123.9, 124.7, 128.4 (CH-Ar), 134.9 (C-6), 139.2 (C-Ar), 150.1 (^{2}C = O), 161.5 (^{4}C = O), 179.7 ppm (C=S). ^{15}N NMR (DMSO-d_6): δ_N = 126.9 (N-1), 131.8 (N-5c), 157.0 ppm (N-3). MS: m/z = 262 (M^+, 40), 228 (100), 185 (12), 169 (15), 157 (15), 103 (50), 77 (15). Anal. Calcd for $C_{11}H_{10}N_4O_2S$ (262.29):C, 50.37; H, 3.84; N, 21.36; S, 12.23. Found: C, 50.46; H, 3.87; N, 21.48; S, 12.31.

3.1.2 1-(2,4-Dioxo-1,2,3,4-tetrahydropyrimidin-5-yl)-3-(*p*-tolyl)thiourea (3b)

Yield: 82%; mp 338–340°C, IR (KBr): υ_{max}/cm^{-1} = 3165 (NH), 2994 (Ar-CH), 1743 (CO), 1668 (CO), 1575 (C=C), 1330, 1210 (C=S). ^{1}H NMR (DMSO-d_6): δ_H = 2.29 (s, 3H, CH_3), 7.14 (d, 2H, J = 8.2 Hz, Ar-H), 8.15 (s, 1H, CH-6), 8.78 (s, 1H, ^{5a}NH), 9.88 (bs, 1H, ^{5c}NH), 10.80 (bs, 1H, ^{1}NH), 11.39 ppm (bs,1H, ^{3}NH). ^{13}C NMR (DMSO-d_6): δ_C = 20.5 (CH_3), 113.3 (C-5), 124.1, 128.8 (CH-Ar), 134.0 (C-6), 136.5 (C-Ar), 150.1 (^{2}C = O), 161.5 (^{4}C = O), 179.7 ppm (C=S). ^{15}N NMR (DMSO-d_6): δ_N = 111.9 (N-5a, 5c), 126.8 (N-1), 156.9 ppm (N-3). MS: m/z = 276 (M^+, 10), 242 (100), 169 (16), 149 (25), 127 (27), 117 (52), 91 (28). Anal. Calcd for $C_{12}H_{12}N_4O_2S$ (276.31): C, 52.16; H, 4.38; N, 20.28; S, 11.60. Found: C, 52.27; H, 4.41; N, 20.36; S, 11.71.

3.1.3 1-(2,4-Dioxo-1,2,3,4-tetrahydropyrimidin-5-yl)-3-(3-methoxyphenyl)thiourea (3c)

Yield: 84%; mp = 350–352°C, IR (KBr) υ_{max}/cm^{-1} = 3164 (NH), 2996 (Ar-CH), 1741 (CO), 1668 (CO), 1574 (C=C), 1330, 1208 (C=S). ^{1}H NMR (DMSO-d_6): δ_H = 3.75 (s, 3H, OCH_3), 6.73 (dd, 1H, J = 8.1, 2.0 Hz, Ar-H), 7.02 (bd, 1H, J = 7.9 Hz, Ar-H), 7.22 (bs, 1H, Ar-H), 7.24 (t, 1H, J = 8.2 Hz, Ar-H), 8.16 (b, 1H, H-6), 8.87 (bs, 1H,^{5c}NH), 10.00 (b, 1H, ^{5a}NH), 10.81 (bs, 1H, ^{1}NH), 11.40 ppm (bs, 1H, ^{3}NH). ^{13}C NMR (DMSO-d_6): δ_C = 55.1 (OCH_3), 109.3, 110.2 (CH-Ar), 113.3 (C-5), 115.7, 129.2 (CH-Ar), 140.3 (C-Ar), 134.9 (C-6), 150.1 (^{2}C = O), 161.5 (^{4}C = O), 179.4 ppm (C=S). MS: m/z = 292 (M^+, 28), 264 (100), 233 (30), 157 (28), 143 (14), 84 (44), 77 (35). ^{15}N NMR (DMSO-d_6): δ_N = 113.5 (N-5c), 126.7 (N-1), 156.9 ppm (N-3). Anal. Calcd for $C_{12}H_{12}N_4O_3S$ (292.31): C, 49.31; H, 4.14; N, 19.17; S, 10.97. Found: C, 49.45; H, 4.17; N, 19.32; S, 10.86.

3.1.4 1-Benzyl-3-(2,4-dioxo-1,2,3,4-tetrahydropyrimidin-5-yl)thiourea (3d)

Yield: 83%; mp = 350–352 (decomp) °C, IR (KBr) υ_{max}/cm^{-1} = 3162 (NH), 2998 (Ar-CH), 1743 (CO), 1668 (CO), 1575 (C=C), 1330, 1210 (C=S). NMR (DMSO-d_6): See Table 1; Figure 3. MS: m/z = 276 (M^+, 24), 244 (100), 171 (20), 157 (35), 143 (20), 98 (41), 91 (48). Anal. Calcd for $C_{12}H_{12}N_4O_2S$ (276.31): C, 52.16; H, 4.38; N, 20.28; S, 11.60. Found: C, 52.27; H, 4.41; N, 20.40; S, 11.72.

3.1.5 1-(2,4-Dioxo-1,2,3,4-tetrahydropyrimidin-5-yl)-3-methylthiourea (3e)

Yield: 85%; mp = 332–334°C, IR (KBr) υ_{max}/cm^{-1} = 3127 (NH), 3086 (Ar-CH), 1689 (CO), 1654 (CO), 1553 (C=C), 1335, 1207 (C=S). ^{1}H NMR (DMSO-d_6): δ_H = 2.85 (d, 3H, J = 4.2 Hz, CH_3), 7.89 (bs, 2H,^{5a}NH, CH-6), 8.53 (bs, 1H, ^{5c}NH), 10.77 ppm (bs, 1H, ^{1}NH), 11.29 ppm (bs, 1H, ^{3}NH). ^{13}C NMR (DMSO-d_6): δ_C = 31.1 (CH_3), 112.7 (C-5), 136.3 (C-6), 150.4 (^{2}C = O), 161.7 (^{4}C = O), 182.1 ppm (C=S). ^{15}N NMR (DMSO-d_6): δ_N = 104.6 (N-5a), 106.1 (N-5c), 127.3 (N-1), 157.0 ppm (N-3). MS: m/z = 200 (M^+, 24), 127 (100), 56 (52). Anal. Calcd for $C_6H_8N_4O_2S$ (200.22): C, 35.99; H, 4.03; N, 27.98; S, 16.02. Found: C, 35.89; H, 4.07; N, 28.05; S, 16.12.

3.1.6 1-Allyl-3-(2,4-dioxo-1,2,3,4-tetrahydropyrimidin-5-yl)thiourea (3f)

Yield: 83%; mp = 348–350 °C (decomp), IR (KBr) υ_{max}/cm^{-1} = 3209 (NH), 3011 (Ar-CH), 1738 (CO), 1667 (CO), 1574 (C=C), 1328, 1205 (C=S). ^{1}H NMR (DMSO-d_6): δ_H = 4.08 (bs, 2H, N-CH_2), 5.07 (d, 1H, J = 10.2, H-5f), 5.17 (dd, 1H, J = 17.2, 1.1 Hz, H-5f), 5.83 (ddt, 1H, J_d = 17.2, 10.4 Hz, J_t = 5.2 Hz, H-5e), 7.98 (b, 1H, H-6), 8.14 (b, 1H; NH-5a), 8.62 (bs, 1H, NH-5c), 10.76 (b, 1H, NH-1), 11.31 ppm (bs, 1H, NH-3). ^{13}C NMR (DMSO-d_6): δ_C = 46.2 (N-CH_2), 112.9 (C-5), 115.5 (C-5f), 134.7 (C-5e, C-6), 150.3 (^{2}C = O), 161.6 (^{4}C = O), 182.4 ppm (C=S). MS: m/z = 226 (M^+, 100), 127 (100), 98 (55), 84 (15), 56 (44). ^{15}N NMR (DMSO-d_6): δ_N = 107.0 (N-5a), 114.9 (N-5c), 157.2 ppm (N-3), Anal. Calcd for $C_8H_{10}N_4O_2S$ (226.26): C, 42.47; H, 4.45; N, 24.76; S, 14.17. Found: C, 42.56; H, 4.48; N, 24.88; S, 14.25.

3.2 General procedure for the synthesis of compounds 5a-l

A solution of **3a-f** (1 mmol) in methanol (20 ml) was added to a 100 ml round bottom flask containing **4a** or **4b** (1.2 mmol) in methanol (10 ml), with refluxing for 4–6 h. After cooling, the yellow precipitate was filtered off, washed with methanol, and recrystallized from a suitable solvent to give pure crystals of **5a-l**.

3.2.1 (*Z*)-Ethyl-2-((*Z*)-2-((2,4-dioxo-1,2,3,4-tetrahydropyrimidin-5-yl)imino)-4-oxo-3-phenyl-thiazolidin-5-ylidene)acetate (5a)

Yield: 76%; mp 320–322°C, IR (KBr) υ_{max}/cm^{-1} = 3147 (NH), 2979 (Ar-CH), 1686 (CO), 1643 (C=N), 1510 (C=C). ^{1}H NMR

(DMSO-d_6): δ_H = 1.24 (t, 3H, J = 6.9 Hz, CH_3), 4.20 (q, 2H, J = 7.0 Hz, CH_2), 6.86 (s, 1H, CH-5a′), 6.92–6.94 (d, 2H, J = 7.8 Hz, Ar-H),7.20–7.23 (t, 2H, J = 7.8 Hz, Ar-H), 7.45–7.47 (d, 2H, J = 7.8 Hz, Ar-H), 8.00 (s, 1H, CH-6), 11.45 (bs, 1H, ^{1}NH), 11.68 ppm (bs, 1H, ^{3}NH). ^{13}C NMR (DMSO-d_6): δ_C = 13.9 (CH_3), 61.6 (OCH_2), 116.5 (C-5′a), 120.7 (C-5), 125.2, 128.2, 129.0, 129.5 (CH-Ar), 134.2 (C-Ar), 140.1 (C-6), 143.7 (C-5′), 147.0 (2C = O), 150.6 (C-2′), 159.8 (C-4), 163.5 (C-4′), 165.2 ppm (C-5′b). MS: m/z = 388 (M+2, 24), 387 (M+1, 100), 386 (M^+, 32), 373 (10), 289 (7), 229 (15), 172 (80), 136 (65). Anal. Calcd for $C_{18}H_{20}N_8O_7S_2$ (524.53): C, 41.22; H, 3.84; N, 21.36; S, 12.23. Found: C, 41.37; H, 3.87; N, 21.43; S, 12.30.

3.2.2 (*Z*)-Ethyl-2-((*Z*)-2-((2,4-dioxo-1,2,3,4-tetrahydropyrimidin-5-yl)imino)-4-oxo-3-(*p*-tolyl)thiazolidin-5-ylidene)acetate (5b)

Yield: 78%; mp 348–350°C, IR (KBr) υ_{max}/cm^{-1} = 3148 (NH), 2979 (Ar-CH), 1686 (CO), 1644 (C=N), 1505 (C=C). ^{1}H NMR (DMSO-d_6): δ_H = 1.24 (t, 3H, J = 7.1 Hz, CH_3), 2.32 (s, 3H, CH_3), 3.28 (s, 3H, NCH_3), 4.22 (q, 2H, J = 7.1 Hz, CH_2), 6.58 (d, 1H, J = 5.2, 0.6 Hz, H-6), 6.83 (d, 2H, J = 8.3 Hz, Ar-H),6.85 (s, 1H, H-5′a), 7.22 (d, 2H, J = 8.00 Hz, Ar-H), 11.05 (bs, 1H, ^{1}NH), 11.42 ppm (bs, 1H, ^{3}NH). ^{13}C NMR (DMSO-d_6): δ_C = 13.9 (C-5d′), 20.5 (CH_3), 61.6 (C-5c′), 108.0 (C-5), 116.4 (C-5a′), 116.4 (C-6), 120.6 (C-*o*), 129.9 (C-*m*), 134.4 (C-*p*), 143.8 (C-*i*), 144.5 (C-2′), 150.6 (C-2), 163.5 (C-4), 161.6 (C-4′), 165.2 ppm (C-5b′). ^{15}N NMR (DMSO-d_6): δ_N = 119.2 (N-1), 155.8 ppm (N-3). MS: m/z = 402 (M+2, 20), 401 (M+1, 85), 400 (M^+, 30), 373 (18), 301 (10), 243 (10), 154 (25), 149 (48), 136 (22), 107 (14), 91 (14). Anal. Calcd for $C_{18}H_{16}N_4O_5S$ (400.41): C, 53.99; H, 4.03; N, 13.99; S, 8.01. Found: C, 53.90; H, 4.06; N, 14.07; S, 8.11.

3.2.3 (*Z*)-Ethyl-2-((*Z*)-2-((2,4-dioxo-1,2,3,4-tetrahydropyrimidin-5-yl)imino)-3-(3-methoxyphenyl)-4-oxo-thiazolidin-5-ylidene) acetate (5c)

Yield: 75%; mp 330–332°C, IR (KBr) υ_{max}/cm^{-1} = 3142 (NH), 2950 (Ar-CH), 1691 (CO), 1648 (C=N), 1598 (C=C). ^{1}H NMR (DMSO-d_6): δ_H = 1.24 (t, 3H, J = 7.1 Hz, H-5d′), 3.76 (s, 3H, OCH_3), 4.22 (q, 2H, J = 7.1 Hz, H-5c′), 6.46 (d, 1H, J = 1.9 Hz, H-2″), 6.51 (d, 1H, J = 8.6 Hz, H-6″), 6.79 (dd, 1H, J = 8.2 Hz, 1.7 Hz, H-4″), 6.86 (s, 1H, H-5a′), 7.32 (dd, 1H, J = 8.1, 8.0 Hz, H-5″), 7.99 (s, 1H, H-5), 11.45 (b, 1H, NH-1), 11.67 ppm (bs, 1H, NH-3). ^{13}C NMR (DMSO-d_6): δ_C = 13.9 (C-5d′), 55.2 (C-3a"), 61.6 (C-5c′), 106.3 (C-2″), 108.0 (C-5), 111.0 (C-4″), 112.7 (C-6″), 116.5 (C-5a"), 130.3 (C-5″), 140.2 (C-5′), 143.7 (C-6), 148.3 (C-1″), 150.6 (C-2′), 150.9 (C-1), 159.8 (C-3″), 160.1 (3″), 163.5 (C-4′), 165.2 ppm (C-5b′). ^{15}N NMR (DMSO-d_6): δ_N = 133.1 (N-1), 158.3 ppm (N-3). MS: m/z = 418 (M+2, 20), 417 (M+1, 84), 416 (M^+, 32), 372 (10), 289 (15), 259 (14), 195 (10), 154 (100), 137 (66), 107 (22). Anal. Calcd for $C_{18}H_{16}N_4O_6S$ (416.41): C, 51.92; H, 3.87; N, 13.45; S, 7.70. Found: C, 51.98; H, 3.85; N, 13.56; S, 7.78.

3.2.4 (*Z*)-Ethyl-2-((*Z*)-3-benzyl-2-((2,4-dioxo-1,2,3,4-tetrahydropyrimidin-5-yl)imino)-4-oxo-thiazolidin-5-ylidene)acetate (5d)

Yield: 85%; mp 314–316°C, IR (KBr) υ_{max}/cm^{-1} = 3150 (NH), 2975 (Ar-CH), 1687 (CO), 1647 (C=N), 1510 (C=C). NMR (DMSO-d_6): See Table 2; Figure 4. MS: m/z = 402 (M+2, 25), 401 (M+1, 100), 400 (M^+, 25), 341 (8), 313 (9), 289 (10), 91 (30). Anal. Calcd for $C_{18}H_{16}N_4O_5S$ (400.41): C, 53.99; H, 4.03; N, 13.99; S, 8.01. Found: C, 53.90; H, 4.06; N, 14.07; S, 8.11.

3.2.5 (*Z*)-Ethyl-2-((*Z*)-2-((2,4-dioxo-1,2,3,4-tetrahydropyrimidin-5-yl)imino)-3-methyl-4-oxo-thiazolidin-5-ylidene)acetate (5e)

Yield: 84%; mp 302–304°C, IR (KBr) υ_{max}/cm^{-1} = 3149 (NH), 3062 (Ar-CH), 1716 (CO), 1674 (CO), 1647 (C=N), 1520 (C=C). ^{1}H NMR (DMSO-d_6): δ_H = 1.25 (t, 3H, J = 6.9 Hz, CH_3), 3.28 (s, 3H, NCH_3), 4.23 (q, 2H, J = 7.0 Hz, CH_2), 6.77 (s, 1H, CH-5′a), 7.25 (s, 1H, CH-6), 10.92 (bs, 1H, ^{1}NH), 11.41 ppm (bs, 1H, ^{3}NH). ^{13}C NMR (DMSO-d_6): δ_C = 13.9 (CH_3), 29.2 (NCH_3), 61.5 (OCH_2), 115.2 (C-5′a), 121.1 (C-5), 131.0 (C-6), 141.0 (C-5′), 150.4 (2C = O), 153.9 (C-2′), 159.6 (C-4), 164.4 (C-4′), 165.3 ppm (C-5b′). ^{15}N NMR (DMSO-d_6): δ_N = 127.0 (N-1), 149.0 (N-3′), 158.2 (N-3), 244.8 ppm (N-5a). MS: m/z = 326 (M+2, 5), 325 (M+1, 30), 324 (M^+, 20), 289 (10), 279 (5), 242 (5), 195 (10). Anal. Calcd for $C_{12}H_{12}N_4O_5S$ (324.31): C, 44.44; H, 3.73; N, 17.28; S, 9.89. Found: C, 44.56; H, 3.80; N, 17.40; S, 9.98.

3.2.6 (*Z*)-Ethyl-2-((*Z*)-3-allyl-2-((2,4-dioxo-1,2,3,4-tetrahydropyrimidin-5-yl)imino)-4-oxo-thiazolidin-5-ylidene)acetate (5f)

Yield: 76%; mp 310–312°C, IR (KBr) υ_{max}/cm^{-1} = 3148 (NH), 2989 (Ar-CH), 1714 (CO), 1675 (CO), 1643 (C=N), 1510 (C=C). ^{1}H NMR (DMSO-d_6): δ_H = 1.25 (t, 3H, J = 7.1 Hz, CH_3), 4.23 (q, 2H, J = 7.1 Hz, OCH_2), 4.44 (d, 2H, J = 5.2 Hz, NCH_2), 5.19 (dd, 1H, J = 10.3 Hz, 1.0 Hz, 3c′CH), 5.21 (dd, 1H, J = 17.2 Hz, 1.1 Hz, CH-3c′), 5.89 (ddt, 1H, J_d = 17.2, 10.4 Hz, Jt = 5.2 Hz, CH-3b′), 6.78 (s, 1H, CH-5a′), 7.27 (d, 1H, J = 6.6 Hz, CH-6), 10.94 (bd, 1H, J = 4.7 Hz, ^{1}NH), 11.40 ppm (bs, 1H, ^{3}NH). ^{13}C NMR (DMSO-d_6): δ_C = 13.9 (CH_3), 44.4 (NCH_2), 61.5 (OCH_2), 115.5 (C-5a′), 117.7 (C-3c′), 120.8 (C-5), 130.9 (C-3b′), 131.3 (C-6), 140.7 (C-5′), 150.4 (C-2), 152.8 (C-2′), 159.5 (C-4), 163.9 (C-4′), 165.2 ppm (C-5b′). ^{15}N NMR (DMSO-d_6): δ_N = 127.3 (N-1), 157.2 (N-3′), 158.1 (N-3), 245.0 ppm (N-4a). MS: m/z = 352 (M+2, 20), 351 (M+1, 100), 350 (M^+, 30), 335 (5), 289 (10), 273 (5), 107 (20). Anal. Calcd for $C_{14}H_{14}N_4O_5S$ (350.35): C, 47.99; H, 4.03; N, 15.99; S, 9.15. Found: C, 47.87; H, 4.07; N, 15.89; S, 9.21.

3.2.7 (*Z*)-Methyl-2-((*Z*)-2-((2,4-dioxo-1,2,3,4-tetrahydropyrimidin-5-yl)imino)-4-oxo-3-phenyl-thiazolidin-5-ylidene)acetate (5g)

Yield: 83%; mp 302–304°C, IR (KBr) υ_{max}/cm^{-1} = 3307, 2975, 1740, 1647. ^{1}H NMR (DMSO-d_6): δ_H = 3.76 (s, 3H, OCH_3), 6.89

(s, 1H, H-5a′), 6.93 (d, 2H, J = 7.4 Hz, Ar-H), 7.22 (t, 1H, J = 7.4 Hz, Ar-H), 7.42 (dd, 2H, J = 8.0, 7.7 Hz, Ar-H), 8.00 (s, 1H, H-6), 11.45 (b, 1H, ^{1}N**H**), 11.67 ppm (b, 1H, ^{3}N**H**). ^{13}C NMR (DMSO-d_6): δ_C = 52.6 (CH_3), 108.0 (C-5), 116.3 (C-5a′), 120.7 (C-*o*), 125.2 (C-*p*), 129.5 (C-*m*), 140.2 (C-5′), 143.8 (C-6), 147.0 (C-*i*), 150.6, 150.7 (C-2, 2′), 159.8 (C-4), 163.5 (C-4′), 165.6 ppm (C-5b′). ^{15}N NMR (DMSO-d_6): δ_N = 133.5 (N-1), 151.4 ppm (N-3). Anal. Calcd for $C_{16}H_{12}N_4O_5S$ (372.36): C, 51.61; H, 3.25; N, 15.05; S, 8.61. Found: C, 51.72; H, 3.28; N, 15.16; S, 8.73.

3.2.8 (*Z*)-Methyl-2-((*Z*)-2-((2,4-dioxo-1,2,3,4-tetrahydropyrimidin-5-yl)imino)-4-oxo-3-(*p*-tolyl)-thiazolidin-5-ylidene)acetate (5h)

Yield: 78%; mp 308–310°C, IR (KBr) υ_{max}/cm^{-1} = 3215 (NH), 3092 (Ar-CH), 1710 (CO), 1679 (CO), 1641 (C=N), 1512 (C=C). ^{1}H NMR (DMSO-d_6): δ_H = 2.32 (s, 3H, CH_3), 3.67 (s, 3H, OCH_3), 6.87 (s, 1H, H-5a′), 7.13–7.15 (m, 4H, Ar-H), 8.00 (s, 1H; H-6), 11.44 (s, 1H, ^{1}NH), 11.66 ppm (b, 1H, ^{3}NH). ^{13}C NMR (DMSO-d_6): δ_C = 20.45 (CH_3), 52.7 (OCH_3), 107.9 (C-5), 116.2 (C-5a′), 120.6, 125.1, 129.9 (CH-Ar), 139.7 (C-5′), 143.8 (C-6), 144.2, 147.0 (C-Ar), 150.5 (C-2), 151.1 (C-2′), 160.0 (C-4), 163.5 (C-4′), 165.6 ppm (C-5b′). MS: m/z = 388 (M+2, 35), 387 (M+1, 100), 386 (M$^+$, 25), 341 (10), 289 (15), 273 (10), 242 (10), 217 (20), 195 (35), 107 (20). Anal. Calcd for $C_{17}H_{14}N_4O_5S$ (386.38): C, 52.84; H, 3.65; N, 14.50; S, 8.30. Found: C, 52.93; H, 3.69; N, 14.61; S, 8.43.

3.2.9 (*Z*)-Methyl-2-((*Z*)-2-((2,4-dioxo-1,2,3,4-tetrahydropyrimidin-5-yl)imino)-3-(3-methoxyphenyl)-4-oxothiazolidin-5-ylidene) acetate (5i)

Yield: 80%; mp 322–324°C, IR (KBr) υ_{max}/cm^{-1} = 3198 (NH), 2998 (Ar-CH), 1711 (CO), 1674 (CO), 1641 (C=N), 1510 (C=C). ^{1}H NMR (DMSO-d_6): δ_H = 3.77 (s, 6H, $2OCH_3$), 6.46 (bs, 1H, Ar-H), 6.51 (d, J = 7.8 Hz, 1H, Ar-H), 6.79 (d, 1H, J = 7.4 Hz, Ar-H), 6.89 (s, 1H, H-5a′), 7.32 (dd, 1H, J = 8.0, 8.0 Hz, Ar-H), 8.00 (bd, 1H, H-6), 11.45 (b, 1H, ^{1}N**H**), 11.67 ppm (bs, 1H, ^{3}N**H**). ^{13}C NMR (DMSO-d_6): δ_C = 52.6 (OCH_3), 55.2 (OCH_3), 106.3 (CH-Ar), 108.0 (C-5), 111.0 (CH-Ar), 112.7 (CH-Ar), 116.3 (C-5a′), 130.4 (CH-Ar), 140.2 (C-5′), 143.7 (C-6), 148.3 (Ar-C), 150.8 (C-1), 150.6 (C-2′), 160.1 (C-4), 159.8 (Ar-C), 163.5 (C-4′), 165.6 ppm (C-5b′). ^{15}N NMR (DMSO-d_6): δ_N = 133.1 (N-1), 158.1 (N-3), 145.5 ppm (N-3′). MS: m/z = 404 (M+2, 25), 403 (M+1, 100), 402 (M$^+$, 38), 391 (5), 273 (10), 274 (15), 258 (30), 167 (32). Anal. Calcd for $C_{17}H_{14}N_4O_6S$ (402.38): C, 50.74; H, 3.51; N, 13.92; S, 7.97. Found: C, 50.86; H, 3.55; N, 13.85; S, 7.85.

3.2.10 (*Z*)-Methyl-2-((*Z*)-3-benzyl-2-((2,4-dioxo-1,2,3,4-tetrahydropyrimidin-5-yl)imino)-4-oxothiazolidin-5-ylidene)acetate (5j)

Yield: 85%; mp 306–308°C, IR (KBr) υ_{max}/cm^{-1} = 3307, 2975, 1740, 1647. NMR (DMSO-d_6): *See* Table 3. MS: m/z = 404 (M+2, 25), 403 (M+1, 100), 402 (M$^+$, 38), 391 (5), 273 (10), 274 (15), 258 (30), 167 (32). Anal. Calcd for $C_{17}H_{14}N_4O_5S$ (386.38): C, 52.84; H, 3.65; N, 14.50; S, 8.30. Found: C, 52.94; H, 3.68; N, 14.62; S, 8.44.

3.2.11 (*Z*)-Methyl-2-((*Z*)-2-((2,4-dioxo-1,2,3,4-tetrahydropyrimidin-5-yl)imino)-3-methyl-4-oxothiazolidin-5-ylidene)acetate (5k)

Yield: 85%; mp 300–302°C, IR (KBr) υ_{max}/cm^{-1} = 3307, 2975, 1740, 1647. ^{1}H NMR (DMSO-d_6): δ_H = 3.27 (s, 3H, NCH_3), 3.77 (s, 3H, OCH_3), 6.80 (s, 1H, H-5a′), 7.24 (d, 1H, J = 5.1 Hz, H-6), 10.92 (bs, 1H, ^{1}N**H**), 11.40 ppm (bs, 1H, ^{3}N**H**). ^{13}C NMR (DMSO-d_6): δ_C = 29.3 (NCH_3), 52.5 (OCH_3), 115.0 (C-5a′), 121.0 (C-5), 131.0 (C-6), 141.0 (C-5'), 150.4 (C-2), 153.8 (C-2′), 159.6 (C-4), 164.4 (C-4′), 165.7 ppm (C-5b′). ^{15}N NMR (DMSO-d_6): δ_N = 127.2 (N-1), 158.0 (N-3), 160.9 ppm (N-3′). Anal. Calcd for $C_{11}H_{10}N_4O_5S$ (310.29): C, 42.58; H, 3.25; N, 18.06; S, 10.33. Found: C, 42.70; H, 3.28; N, 18.15; S, 10.44.

3.2.12 (*Z*)-Methyl-2-((*Z*)-3-allyl-2-((2,4-dioxo-1,2,3,4-tetrahydropyrimidin-5-yl)imino)-4-oxothiazolidin-5-ylidene)acetate (5l)

Yield: 78%; mp 314–316°C, IR (KBr) υ_{max}/cm^{-1} = 3147 (NH), 2999 (Ar-CH), 1710 (CO), 1675 (CO), 1644 (C=N), 1511 (C=C). ^{1}H NMR (DMSO-d_6): δ_H = 3.77 (s, 3H, OCH_3), 4.21 (d, 2H, J = 5.2 Hz, NCH_2), 5.19 (dd, 1H, J = 10.3 Hz, 1.0 Hz, 3c′CH), 5.22 (dd, 1H, J = 17.2 Hz, 1.1 Hz, CH-3c′), 5.80 (ddt, 1H, Jd = 17.2, 10.4 Hz, Jt = 5.2 Hz, CH-3b′), 6.75 (s, 1H, CH-5a′), 7.24 (d, 1H, J = 6.6 Hz, CH-6), 10.89 (bs, 1H, ^{1}N**H**), 11.42 ppm (bs, 1H, ^{3}N**H**). ^{13}C NMR (DMSO-d_6): δ_C = 42.6 (NCH_2), 53.6 (OCH_3), 116.1 (C-5a′), 116.5 (C-3c′), 120.6 (C-5), 130.0 (C-3b′), 134.4 (C-6), 140.3 (C-5′), 150.3 (C-2), 150.6 (C-2′), 159.8 (C-4), 163.5 (C-4′), 165.6 ppm (C-5b′). MS: m/z = 336 (M$^+$, 35), 321 (20), 305 (10), 273 (5), 277 (14), 250 (25), 125 (100). Anal. Calcd for $C_{13}H_{12}N_4O_5S$ (336.32): C, 46.43; H, 3.60; N, 16.66; S, 9.53. Found: C, 46.56; H, 3.64; N, 16.75; S, 9.66.

4 Biology

Supplementary Appendix SA contains information on all biological assay tests.

5 Conclusion

Due to the importance of thiazolidinone-pyrimidine derivatives, we direct for the synthesis of 2,4-dioxo-1,2,3,4-tetrahydropyrimidin-5-yl)imino)-4-oxo-3-yl-thiazolidin-5-ylidene)acetates **5a-l** through the reaction of thioureas **3a-f** with diethyl/dimethyl acetylenedicarboxylates (**4a,b**). The

structure of compounds was examined by ^{1}H, ^{13}C-NMR, 2D-NMR, and ^{15}N-NMR spectroscopy and elemental analyses. Compounds **5b** and **5j** were the most potent EGFR and $BRAF^{V600E}$ inhibitors and could be used as dual EGFR and $BRAF^{V600E}$ inhibitors with promising antiproliferative properties. Moreover, the synthesized molecules were *in-silico* inspected towards EGFR and $BRAF^{V600E}$ as anticarcinoma drug candidates using AUTODOCK4.2.6 software. Based on docking scores, compounds **5b** and **5j** disclosed auspicious docking scores towards EGFR and $BRAF^{V600E}$. These findings shed new light on the importance of compounds **5b** and **5j** as appropriate therapeutic treatments for cancer disease.

Data availability statement

The original contributions presented in the study are included in the article/Supplementary Material, further inquiries can be directed to the corresponding authors.

Author contributions

CRediT authorship contribution statement. MA: editing and revision. ASA: Conceptualization, writing, and editing. BY: Biology, methodology, writing, and editing, AB: NMR, editing. AKA: editing. SB: Editing and revision; AM: Conceptualization, writing, methodology, editing and writing the draft.

Acknowledgments

The authors thank the Deanship of Scientific Research at Prince Sattambin Abdulaziz University under research project No 2021/01/18104. We also acknowledge support from the KIT-Publication Fund of the Karlsruhe Institute of Technology.

Conflict of interest

The authors declare that the research was conducted in the absence of any commercial or financial relationships that could be construed as a potential conflict of interest.

Publisher's note

All claims expressed in this article are solely those of the authors and do not necessarily represent those of their affiliated organizations, or those of the publisher, the editors and the reviewers. Any product that may be evaluated in this article, or claim that may be made by its manufacturer, is not guaranteed or endorsed by the publisher.

Supplementary material

The Supplementary Material for this article can be found online at: https://www.frontiersin.org/articles/10.3389/fchem.2022.1076383/full#supplementary-material

References

Abbas, S. Y., Farag, A. A., Ammar, Y. A., Atrees, A. A., Mohamed, A. F., and El-Henawy, A. A. (2013a). Synthesis, characterization, and antiviral activity of novel fluorinated isatin derivatives. *Monatsh. Chem.* 144, 1725–1733. doi:10.1007/s00706-013-1034-3

Abbas, S. Y., El-Sharief, M. A. M. S., Basyouni, W. M., Fakhr, I. M. I., and El-Gammal, E. W. (2013b). Thiourea derivatives incorporating a hippuric acid moiety: Synthesis and evaluation of antibacterial and antifungal activities. *Eur. J. Med. Chem.* 64, 111–120. doi:10.1016/j.ejmech.2013.04.002

Abdelrahman, M. H., Aboraia, H. S., Youssif, B. G. M., and Elsadek, B. E. M. (2017). Design, synthesis and pharmacophoric model building of new 3-alkoxymethyl/3-phenyl indole-2-carboxamides with potential antiproliferative activity. *Chem. Biol. Drug Des.* 90, 64–82. doi:10.1111/cbdd.12928

Alshammari, M. B., Aly, A. A., Bräse, S., Nieger, M., and Abd El-Haleem, L. E. (2022). Efficient synthesis of various substituted (thio)ureas, semicarbazides, thiosemicarbazides, thiazolidones, and oxadiazole derived from [2.2] paracyclophane. *ACS Omega* 7, 12879–12890. doi:10.1021/acsomega.2c00141

Al-Wahaibi, L. H., Gouda, A. M., Abou-Ghadir, O. F., Salem, O. I. A., Ali, A. T., Farghaly, H. S., et al. (2020). Design and synthesis of novel 2, 3-dihydropyrazino[1, 2-*a*]indole-1, 4-dione derivatives as antiproliferative EGFR and $BRAF^{V600E}$ dual inhibitors. *Bioorg. Chem.* 104, 104260. doi:10.1016/j.bioorg.2020.104260

Aly, A. A., Bräse, S., Hassan, A. A., Mohamed, N. K., Abd El-Haleem, L. E., Nieger, M., et al. (2020). New paracyclophanyl-thiazoles of *anti*-leukemia activity; design, synthesis, molecular docking, and mechanistic study. *Molecules* 25, 3089. doi:10.3390/molecules25133089

Asati, V., Mahapatra, D. K., and Bharti, S. K. (2014). Thiazolidine-2, 4-diones as multi-targeted scaffold in medicinal chemistry: Potential anticancer agents. *Eur. J. Med. Chem.* 87, 814–833. doi:10.1016/j.ejmech.2014.10.025

Aziz, M. W., Kamal, A. M., Mohamed, K. O., and Elgendy, A. A. (2021). Design, synthesis, and assessment of new series of quinazolinone derivatives as EGFR inhibitors along with their cytotoxic evaluation against MCF7 and A549 cancer cell lines. *Bioorg. Med. Chem. Lett.* 41, 127987. doi:10.1016/j.bmcl.2021.127987

Baraldi, P. G., Romagnoli, R., Guadix, A. E., Pineda de las Infantas, M. J., Gallo, M. A., Espinosa, A., et al. (2002). Design, synthesis, and biological activity of hybrid compounds between uramustine and DNA minor groove binder distamycin A. *J. Med. Chem.* 45, 3630–3638. doi:10.1021/jm011113b

Bollag, G., Hirth, P., Tsai, J., Zhang, J., Ibrahim, P. N., Cho, H., et al. (2010). Clinical efficacy of a RAF inhibitor needs broad target blockade in BRAF-mutant melanoma. *Nature* 467, 596–599. doi:10.1038/nature09454

Bouhadir, K. H., Koubeissi, A., Mohsen, F. A., El-Harakeh, M. D., Cheaib, R., Younes, J., et al. (2016). Novel carbocyclic nucleoside analogs suppress glomerular mesangial cells proliferation and matrix protein accumulation through ROS-dependent mechanism in the diabetic milieu. II. Acylhydrazone-functionalized pyrimidines. *Bioorg. Med. Chem. Lett.* 26, 1020–1024. doi:10.1016/j.bmcl.2015.12.042

Dassault Systèmes (2019). *BIOVIA, B.D.S.V.; Version 2019*. San Diego, CA, USA: Dassault Systèmes BIOVIA.

El-Sharief, M. A. M. S., Abbas, S. Y., El-Bayouki, K. A. M., and El-Gammal, E. W. (2013). Synthesis of thiosemicarbazones derived from *N*-(4-hippuric acid)-thiosemicarbazide and different carbonyl compounds as antimicrobial agents. *EurJ. Med. Chem.* 67, 263–268. doi:10.1016/j.ejmech.2013.06.031

El-Sharief, H. A. M., Youssif, B. G. M., Bukhari, S. N. A., Abdel-Aziz, M., and Abdel-Rahman, H. M. (2018). Novel 1, 2, 4-triazole derivatives as potential anticancer agents: Design, synthesis, molecular docking, and mechanistic studies. *Bioorg. Chem.* 76, 314–325. doi:10.1016/j.bioorg.2017.12.013

Gimadieva, A. R., Khazimullina, Yu.Z., Belaya, E. A., Zimin, Yu.S., Abdrakhmanov, L. B., and Mustafin, A. G. (2015). Express evaluation of antioxidant activity of uracil derivatives. *Biomed. Khim.* 61, 765–769. doi:10.18097/pbmc20156106765

Gomaa, H. A. M., Shaker, M. E., Alzarea, S. I., Hendawy, O. M., Mohamed, F. A. M., Gouda, A. M., et al. (2022). Optimization and SAR investigation of novel 2, 3-dihydro-pyrazino[1, 2-*a*]indole-1, 4-dione derivatives as EGFR and $BRAF^{V600E}$ dual inhibitors with potent antiproliferative and antioxidant activities. *Bioorg. Chem.* 120, 105616. doi:10.1016/j.bioorg.2022.105616

Goodford, P. J. (1985). A computational procedure for determining energetically favorable binding sites on biologically important macromolecules. *J. Med. Chem.* 28, 849–857. doi:10.1021/jm00145a002

Huang, H., Chen, Q., Xin, K., Meng, L., Lin, L., Wang, X., et al. (2010). A series of alpha-heterocyclic carboxaldehyde thiosemicarbazones inhibit topoisomerase IIα catalytic activity. *J. Med. Chem.* 53, 3048–3064. doi:10.1021/jm9014394

Ibrahim, M. A. A., Abdeljawaad, K. A. A., Abdelrahman, A. H. M., Jaragh-Alhadad, L. A., Oraby, H. F., Elkaeed, E. B., et al. (2022a). Exploring natural product activity and species source candidates for hunting ABCB1 transporter inhibitors: An *in silico* drug discovery study. *Molecules* 27, 3104. doi:10.3390/molecules27103104

Ibrahim, M. A. A., Badr, E. A. A., Abdelrahman, A. H. M., Almansour, N. M., Mekhemer, G. A. H., Shawky, A. M., et al. (2022b). *In silico* targeting human multidrug transporter ABCG2 in breast cancer: Database screening, molecular docking, and molecular dynamics study. *Mol. Inf.* 41, 2060039. doi:10.1002/minf.202060039

Isobe, Y., Tobe, M., Inoue, Y., Isobe, M., Tsuchiya, M., and Hayashi, H. (2003). Structure and activity relationships of novel uracil derivatives as topical anti-inflammatory agents. *Bioorg. Med. Chem.* 11, 4933–4940. doi:10.1016/j.bmc.2003.09.012

Krutikov, V. I., and Erkin, A. V. (2009). 5-Arylideneaminouracils: II. Synthesis of sodium and ammonium salts. *Russ. J. Gen. Chem.* 79, 991–995. doi:10.1134/s1070363209050211

Lee, B.-H., Shin, J.-H., Lim, M.-K., Jang, T.-S., Park, J.-S., Kim, K.-H., et al. (1997). Partition property of 5-nitrothiopyrimidine nucleoside. *Bull. Kor. Chem. Soc.* 18, 734–736. doi:10.5012/bkcs.1997.18.7.734

Li, H.-Q., Yan, T., Yang, Y., Shi, L., Zhou, C.-F., and Zhu, H.-L. (2010). Synthesis and structure–activity relationships of *N*-benzyl-*N*-(X-2-hydroxybenzyl)-*N′*-phenylureas and thioureas as antitumor agents. *Bioorg. Med. Chem.* 18, 305–313. doi:10.1016/j.bmc.2009.10.054

Mahmoud, M. A., Mohammed, A. F., Salem, O. I. A., Gomaa, H. A. M., and Youssif, B. G. M. (2022). New 1, 3, 4-oxadiazoles linked with the 1, 2, 3-triazole moiety as antiproliferative agents targeting the EGFR tyrosine kinase. *Arch. Pharm.* 355, 2200009. doi:10.1002/ardp.202200009

Mohamed, F. A. M., Gomaa, H. A. M., Hendawy, O. M., Ali, A. T., Farghaly, H. S., Gouda, A. M., et al. (2021). Design, synthesis, and biological evaluation of novel EGFR inhibitors containing 5-chloro-3-hydroxymethyl-indole-2-carboxamide scaffold with apoptotic antiproliferative activity. *Bioorg. Chem.* 112, 104960. doi:10.1016/j.bioorg.2021.104960

Mohassab, A. M., Hassan, H. A., Abdelhamid, D., Gouda, A. M., Youssif, B. G. M., Tateishi, H., et al. (2021). Design and synthesis of novel quinoline/chalcone/1, 2, 4-triazole hybrids as potent antiproliferative agent targeting EGFR and $BRAF^{V600E}$ kinases. *Bioorg. Chem.* 106, 104510. doi:10.1016/j.bioorg.2020.104510

Morris, G. M., Huey, R., Lindstrom, W., Sanner, M. F., Belew, R. K., Goodsell, D. S., et al. (2009). AutoDock4 and AutoDockTools4: Automated docking with selective receptor flexibility. *J. Comput. Chem.* 30, 2785–2791. doi:10.1002/jcc.21256

Napper, A. D., Hixon, J., McDonagh, T., Keavey, K., Pons, J.-F., Barker, J., et al. (2005). Discovery of indoles as potent and selective inhibitors of the deacetylase SIRT1. *J. Med. Chem.* 48, 8045–8054. doi:10.1021/jm050522v

Oliev, R. (1994). Response to auxin by cells of *Riella helicophylla* during reversible arrest in different cell-cycle phases. *Planta* 194, 510–515. doi:10.1007/bf00714464

Palasz, A., and Ciez, D. (2015). In search of uracil derivatives as bioactive agents. Uracils and fused uracils: Synthesis, biological activity and applications. *Eur. J. Med. Chem.* 97, 582–611. doi:10.1016/j.ejmech.2014.10.008

Putz, M. V., and Dudas, N. A. (2013). Variational principles for mechanistic quantitative structure–activity relationship (QSAR) studies: Application on uracil derivatives' anti-HIV action. *Struct. Chem.* 24, 1873–1893. doi:10.1007/s11224-013-0249-6

Rana, V. S., and Ganesh, K. N. (2000). Recognition of 5-aminouracil (U^{a}) in the central strand of a DNA triplex: Orientation selective binding of different third strand bases. *Nucleic Acids Res.* 28, 1162–1169. doi:10.1093/nar/28.5.1162

Roth, B., and Cheng, C. C. (1982). Recent progress in the medicinal chemistry of 2, 4-diaminopyrimidines. *Prog. Med. Chem.* 19, 269–331. doi:10.1016/s0079-6468(08)70332-1

Seferoglu, Z., and Ertan, N. (2008). Synthesis, characterization and spectroscopic properties of some new phenylazo-6-aminouracil. *Open Chem.* 6, 81–88. doi:10.2478/s11532-007-0062-4

Sharma, P. C., Bansal, K. K., Sharma, A., Sharma, D., and Deep, A. (2020). Thiazole-containing compounds as therapeutic targets for cancer therapy. *Eur. J. Med. Chem.* 188, 112016. doi:10.1016/j.ejmech.2019.112016

Stamos, J., Sliwkowski, M. X., and Eigenbrot, C. (2002). Structure of the epidermal growth factor receptor kinase domain alone and in complex with a 4-anilinoquinazoline inhibitor. *J. Biol. Chem.* 277, 46265–46272. doi:10.1074/jbc.m207135200

Tanase, C. I., Draghici, C., Cojocaru, A., Galochkina, A. V., Orshanskaya, J. R., Zarubaev, V. V., et al. (2015). New carbocyclic N^{6}-substituted adenine and pyrimidine nucleoside analogues with a bicyclo[2.2.1]heptane fragment as sugar moiety; synthesis, antiviral, anticancer activity and X-ray crystallography. *Bioorg. Med. Chem.* 23, 6346–6354. doi:10.1016/j.bmc.2015.08.033

Xiong, X., Liu, H., Fu, L., Li, L., Li, J., Luo, X., et al. (2008). Antitumor activity of a new N-substituted thiourea derivative, an EGFR signaling-targeted inhibitor against a panel of human lung cancer cell lines. *Chemotherapy* 54, 463–474. doi:10.1159/000159272

Youssif, B. G. M., Mohamed, A. M., Osman, E. E. A., Abou-Ghadir, O. F., Elnaggar, D. H., Abdelrahman, M. H., et al. (2019). 5-Chlorobenzo-furan-2-carboxamides: From allosteric CB1 modulators to potential apoptotic antitumor agents. *Eur. J. Med. Chem.* 177, 1–11. doi:10.1016/j.ejmech.2019.05.040

Ziegler-Skylakakis, K., Rossberger, S., and Andrae, U. (1985). Thiourea induces DNA repair synthesis in primary rat hepatocyte cultures and gene mutations in V79 Chinese hamster cells. *Arch. Toxicol.* 58, 5–9. doi:10.1007/bf00292608

Zielenkiewicz, W., Poznanski, J., and Zielenkiewicz, A. (2000). Partial molar volumes of aqueous solutions of some halo and amino derivatives of uracil. *J. Solut. Chem.* 29, 757–769. doi:10.1023/a:1005169112192